Ultrasonics 58 (2015) 96–103

Contents lists available at ScienceDirect

Ultrasonics

journal homepage: www.elsevier.com/locate/ultras

The application of second-order approximation of Taylor series in thickness shear vibration analysis of quartz crystal microbalances

Peng Li [a], Feng Jin [b,*], Qing Sun [a], Jianxun Ma [a]

[a] School of Human Settlements and Civil Engineering, Xi'an Jiaotong University, Xi'an 710049, China
[b] State Key Laboratory for Strength and Vibration of Mechanical Structures, School of Aerospace, Xi'an Jiaotong University, Xi'an 710049, China

ARTICLE INFO

Article history:
Received 1 June 2014
Received in revised form 27 December 2014
Accepted 29 December 2014
Available online 6 January 2015

Keywords:
Thickness shear vibration
Second-order approximation
Frequency shift
Admittance analysis
Transient effect

ABSTRACT

The inertia force caused by an additional mass layer is usually adopted to simulate the effective mechanical boundary condition in a quartz crystal microbalance (QCM), which may yield incorrect results when the upper layer becomes relative thicker. Thus, a detail analysis of the thickness shear vibration in a QCM for detecting the characteristics of the upper isotropic layer is proceeded based on a second-order approximation of Taylor series. The result calculated by this method has a higher accuracy than that of inertial-force approximation. According to these outcomes, the free and forced vibration has been illustrated, as well as transient effects during the switching on/off processes or under a sudden fluctuation of the driving-voltage amplitude or frequency. It has been revealed by numerical simulation that the additional mass layer has a great influence on the mechanical performance of QCM, including the resonance frequency, amplitudes of displacement and admittance, response time of the transient processes, and so on. These findings can prove effective guidance for physical phenomenon explanations and experimental measurement in mass sensor devices.

1. Introduction

Owning to its advantage of high sensitivity and distinguishability, the quartz crystal microbalance (QCM) has been regarded as very convenient to detect physical property changes of thin layers at its surfaces, which has been widely used in many regions, such as physics, biology, chemistry and medicine [1]. By changing the quality of the material under test into frequency signal, QCM can be applied to measure the properties of affiliated layer [2]. Sometimes, the resonance frequency can be reached gigahertz, with its thickness typically in the range of some micro-meters. Hence, it is easy to measure mass densities of the attached layer down to a level of 1 μg/cm^2 [3,4].

The frequency of oscillation, which is partially dependent on the thickness of the mass layer, is the basic performance index of the QCM. During the past decades, the effect of some mechanical characteristics on resonance frequency of QCM have been extensively investigated, including visco-elasticity [1], inhomogeneity of mass layer [5], imperfection of connected interface [6], electrical admittance [7], and so on. Among these explorations mentioned above, an inertia force caused by the thin layer is usually applied for the description of mechanical boundary condition at the upper surface of the crystal plate [5,8,9], which replaces a detailed analysis of mechanical and electrical coupling. Based on this simplification, Sauerbrey's equation provides a simple computational formula about resonance frequency, which is proportional to the mass of the film attached [1]. However, it has been pointed that this kind of simplification may yield incorrect results especially when the upper layer becomes relative thicker [10]. Both the mass and stiffness effects must be considered during the analysis. Hence, the present paper will introduce a second-order approximation of Taylor series, which will be more accurate than the previous inertial-force approximation.

On the other hand, owning to the piezoelectricity of AT-cut crystal plate, an alternative voltage applied on its two surfaces is usually used to excite a particular vibration mode. Another phenomenon, transient effect [11,12], is inevitable during the excitation process of QCM. For instance, the initial switching-on from rest, followed by a sudden switching-off caused by the interruption of incident current, fluctuations in the driving voltage or the frequency, and thermal and mechanical shocks, and so forth. They can disturb resonator operation evidently. There have been a few attempts to study the transient effect on the thickness-shear vibration in quartz crystal resonators [13–15]. However, the theoretical model mentioned above is simplified as a single infinite piezoelectric plate. To the best of our knowledge, little work has been

* Corresponding author. Fax: +86 29 82667091.
E-mail address: jinfengzhao@263.net (F. Jin).

http://dx.doi.org/10.1016/j.ultras.2014.12.007
0041-624X/

performed so far to discuss the transient effect in the composite layered structures, which contains at least two different materials. However, this is significant for the design of high-quality electronic devices.

Synthesis above, a systematic investigation, including resonance frequency solving, forced vibration analysis, and some transient responses, on the thickness shear vibration performance of QCM is carried out in present contribution by using of a second-order approximation of Taylor series. The dispersion equation has been obtained from linear elastic theory, which can be reduced to a few known elastic or quasi-static piezoelectric solutions. Based on this equation, the effect of affiliated mass layer on some property indices of thickness shear mode, such as resonance frequency, displacement distribution, admittance amplitude, and transient response time, has been revealed numerically. Finally, some conclusions are given.

2. Thickness-shear vibration analysis

QCM is inexpensive owning to its simple configuration. For our purpose it is sufficient to consider an AT-cut quartz plate having a thickness of $2h$ and a mass density ρ in Fig. 1. Meanwhile, an additional mass layer with its thickness and mass density being $2h'$ and ρ' respectively is perfectly bonded on its upper surface. The origin of coordinates is set on the middle plane of the AT-cut quartz plate without loss of generality. Meanwhile, the alternating voltage $\pm V\exp(i\omega t)$ which are respectively imposed on the upper and bottom surfaces of the crystal plate, i.e., $x_2 = \pm h$, are used to excite the thickness shear vibration. Here, ω is the circular frequency, t stands for time, and $i^2 = -1$. Generally speaking, the thickness shear vibration may be coupled to flexure and face shear motions, and this kind of coupling depends on the plate dimensions [16]. It has been revealed that at certain length/thickness ratio, thickness shear vibration can be excited independently [16]. Hereby, the displacement vector $\boldsymbol{u}$ and electric potential φ in the AT-cut crystal plate can be described by

$$u_1 = u_1(x_2, t), \quad u_2 = u_3 = 0, \quad \varphi = \varphi(x_2, t). \tag{1}$$

By virtue of constitutive and geometric relations, dynamic equations and Maxwell's law, the governing equations corresponding to u_1 and φ are

$$\begin{cases} c_{66}\frac{\partial^2 u_1}{\partial x_2^2} + e_{26}\frac{\partial^2 \varphi}{\partial x_2^2} = \rho\frac{\partial^2 u_1}{\partial t^2}, \\ e_{26}\frac{\partial^2 u_1}{\partial x_2^2} - \varepsilon_{22}\frac{\partial^2 \varphi}{\partial x_2^2} = 0. \end{cases} \tag{2}$$

where c_{66}, e_{26}, ε_{22} are the elastic and piezoelectric coefficients and dielectric permittivity, respectively. The thickness shear vibration solution in the AT-cut quartz plate can also be expressed as [4,6,10]

$$\begin{cases} u_1 = [A_1\cos(\xi x_2) + A_2\sin(\xi x_2)]\exp(i\omega t), \\ \varphi = \left\{\frac{e_{26}}{\varepsilon_{22}}[A_1\cos(\xi x_2) + A_2\sin(\xi x_2)] + (A_3 x_2 + A_4)\right\}\exp(i\omega t). \end{cases} \tag{3}$$

in which A_1, A_2, A_3, and A_4 are undetermined coefficients, and $\xi = \frac{\omega}{\sqrt{c_{66}/\rho}}$ is the wave number with the relative piezoelectric stiffness $\bar{c}_{66} = c_{66} + \frac{e_{26}^2}{\varepsilon_{22}}$. Hence, the corresponding stress and electric displacement components are:

$$\begin{cases} T_{12} = \{\bar{c}_{66}\xi[-A_1\sin(\xi x_2) + A_2\cos(\xi x_2)] + e_{26}A_3\}\exp(i\omega t), \\ D_2 = -\varepsilon_{22}A_3\exp(i\omega t). \end{cases} \tag{4}$$

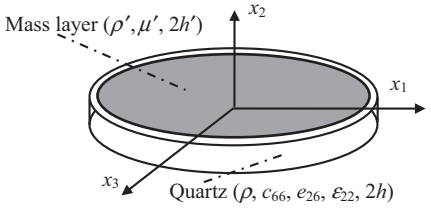

Fig. 1. A quartz crystal microbalance with an additional mass layer on its surface.

Once the thickness shear mode is excited, the mass layer will vibrates following the plate's motion with its displacement components being

$$u_1' = u_1'(x_2, t), \quad u_2' = u_3' = 0. \tag{5}$$

where $\boldsymbol{u}'$ stands for the displacement vector of the attached mass layer. Based on Eq. (5), the stress component T_{12}' and equilibrium equation can be obtained as:

$$T_{12}' = \mu'\frac{\partial u_1'}{\partial x_2}, \ \frac{\partial T_{12}'}{\partial x_2} = \rho'\frac{\partial^2 u_1'}{\partial t^2}, \tag{6}$$

with μ' representing elastic coefficient of the mass layer. By using of Eq. (6), we can get the following relation

$$\frac{\partial}{\partial x_2}\boldsymbol{R} = \boldsymbol{M}\boldsymbol{R}. \tag{7}$$

where $\boldsymbol{R} = \begin{bmatrix} u_1' \\ T_{12}' \end{bmatrix}$, and $\boldsymbol{M} = \begin{bmatrix} 0 & \frac{1}{\mu'} \\ \rho'\frac{\partial^2}{\partial t^2} & 0 \end{bmatrix}$. Furthermore,

$$\frac{\partial^n}{\partial x_2^n}\boldsymbol{R} = \boldsymbol{M}^n\boldsymbol{R}, \ \text{with } n = 1, 2, 3, \ldots. \tag{8}$$

A quartz crystal microbalance is widely used to measure the characteristics of an additional thin layer upon its surface by calculating the frequency shift. Specifically, the layer is so thin compared with the quartz plate, i.e., let $2h'$ be small, that we can expand the expression of stress T_{12}' at $x_2 = (h + 2h')$ into Taylor series at $x_2 = h$ [8,17]:

$$T_{12}'(h + 2h') = T_{12}'(h) + 2h'\frac{\partial}{\partial x_2}T_{12}'(h) + \frac{(2h')^2}{2!}\frac{\partial^2}{\partial x_2^2}T_{12}'(h) + \frac{(2h')^3}{3!}\frac{\partial^3}{\partial x_2^3}T_{12}'(h) + \ldots \tag{9}$$

In present contribution, we only consider the second-order approximation of Taylor series for simplification. Owning to the fact that the top surface of mass layer is traction free, i.e., $T_{12}'(h + 2h') = 0$, substituting Eq. (9) into Eq. (8) yields

$$\left[1 - 2(\xi' h')^2\right]T_{12}'(h) - 2h'\rho'\omega^2 u_1'(h) = 0. \tag{10}$$

where $\xi' = \frac{\omega}{\sqrt{\mu'/\rho'}}$ is the wave number of the layer. If we only consider the first-order approximation in Eq. (9), i.e., the terms containing h'^2 should be zero, Eq. (10) can be degenerated as

$$T_{12}'(h) = 2h'\rho'\omega^2 u_1'(h). \tag{11}$$

which is the boundary condition that is usually used in previous research [1,9], i.e., only considering the inertial force caused by the mass layer. In this paper, we will discuss the performance of QCM based on the second-order approximation described by Eq. (10) that is more accurate than those previous works.

The other boundary conditions at $x_2 = \pm h$ requires

$$T_{12}(-h) = 0, \quad \varphi(-h) = -V. \tag{12}$$

$$T_{12}(h) = T_{12}'(h), \quad u_1(h) = u_1'(h), \quad \varphi(h) = V. \tag{13}$$

Substituting the displacement and stress expressions, i.e., Eqs. (3) and (4), into the above boundary conditions, i.e., Eqs. (10), (12) and (13), yields four linear homogeneous algebraic equations for coefficients A_1, A_2, A_3, and A_4:

$$\bar{c}_{66}\xi[A_1\sin(\xi h) + A_2\cos(\xi h)] + e_{26}A_3 = 0, \tag{14a}$$

$$[1-2(\xi' h')^2]\{\bar{c}_{66}\xi[-A_1\sin(\xi h)+A_2\cos(\xi h)]+e_{26}A_3\} - 2h'\rho'\omega^2[A_1\cos(\xi h)+A_2\sin(\xi h)]=0, \tag{14b}$$

$$\frac{e_{26}}{\varepsilon_{22}}[A_1\cos(\xi h)+A_2\sin(\xi h)]+A_3 h+A_4=V, \tag{14c}$$

$$\frac{e_{26}}{\varepsilon_{22}}[A_1\cos(\xi h)-A_2\sin(\xi h)]-A_3 h+A_4=-V. \tag{14d}$$

These undermined coefficients A_1, A_2, A_3, and A_4 can be deduced as

$$A_1=-\frac{e_{26}V}{\bar{c}_{66}}\frac{2\xi h R_0\sin(\xi h)}{\Delta},\quad A_2=-\left\{\cot(\xi h)+\frac{1}{\xi h R_0}[1-2(\xi' h')^2]\right\}A_1,$$
$$A_3=-\frac{\bar{c}_{66}}{e_{26}}\xi[A_1\sin(\xi h)+A_2\cos(\xi h)],\quad A_4=-\frac{e_{26}}{\varepsilon_{22}}\cos(\xi h)A_1. \tag{15}$$

where

$$\Delta=2\sin(\xi h)\left[1-2(\xi' h')^2\right]\left[k_{26}^2\sin(\xi h)-\xi h\cos(\xi h)\right] + \xi h R_0\left[k_{26}^2\sin(2\xi h)-2\xi h\cos(2\xi h)\right], \tag{16}$$

and $R_0=\frac{2h'\rho'}{2h\rho}=\frac{\mu'\xi'}{\bar{c}_{66}\xi}\frac{2h'\xi'}{2h\xi}$. $\Delta=0$ yields the resonance frequency equation of thickness shear vibration in the QCM in Fig. 1 when the upper and bottom surfaces of the crystal plate are electrically shorted (i.e., without the initial voltage $V=0$), which is related to the free vibration of such composites.

$$2\sin(\xi h)\left[1-2(\xi' h')^2\right]\left[k_{26}^2\sin(\xi h)-\xi h\cos(\xi h)\right] + \xi h R_0\left[k_{26}^2\sin(2\xi h)-2\xi h\cos(2\xi h)\right]=0. \tag{17}$$

Supposing that there is no additional mass layer on the surface of quartz crystal plate, i.e., $h'=0$, Eq. (17) can be degenerated as

$$\tan(\xi h)\left[k_{26}^2\tan(\xi h)-\xi h\right]=0. \tag{18}$$

That is just the result by Tiersten [18] and Yang et al. [10,19]. Besides, if only the inertia effect of mass layer is considered, i.e., the polynomial containing h'^2 is neglected, the frequency equation can be abbreviated as

$$\left[2k_{26}^2\frac{\sin^2(\xi h)}{\cos(2\xi h)}-\xi h\tan(2\xi h)\right]+\xi h R_0\left[k_{26}^2\tan(2\xi h)-2\xi h\right]=0. \tag{19}$$

Furthermore, owning to the fact that the electro-mechanical coupling effect of quartz crystal is weak, for example, $k_{26}^2=0.78\%$, we can ignore this parameter and get

$$\frac{\mu'\xi'}{\bar{c}_{66}\xi}(2\xi' h')+\tan(2\xi h)=0. \tag{20}$$

Because the additional mass layer is so thin, that the approximation of $\tan(2\xi' h')\approx 2\xi' h'$ can be used. Hence, the frequency equation is equivalent to the following form:

$$\frac{\mu'\xi'}{\bar{c}_{66}\xi}\tan(2\xi' h')+\tan(2\xi h)=0, \tag{21}$$

which is the same as our previous work [20]. The two points above can validate the accuracy of our theoretical derivation to a certain extent.

3. Numerical simulations

For a numerical example, an AT-cut quartz plate with the thickness $2h=1$ mm, elastic constant $c_{66}=2.901\times10^{10}$ N/m^2, piezoelectric coefficient $e_{26}=0.095$ C/m^2, dielectric permittivity $\varepsilon_{22}=3.982\times10^{-11}$ F/m, and mass density $\rho=2649$ kg/m^3 is considered [21]. In Fig. 1, infinite wave modes can be excited by the alternative voltage, and we mainly discuss the fundamental thickness shear mode in the following analysis. Generally speaking, Eq. (17) is a transcendental equation, in which the frequency cannot be solved using an explicit expression. Hence, we have adopted the bisection method for numerical computations [22].

3.1. Resonance frequency

Fig. 2 gives the frequency comparison of the fundamental mode respectively calculated by second-order approximation, i.e., Eq. (17), first-order approximation, i.e., Eq. (19), and exact solution, i.e., Eq. (A3) in Appendix A, with the mass density and elasticity satisfying $\rho'=\rho$, and $\mu'=c_{66}$. Meanwhile, $\omega_s=\frac{\pi}{2h}\sqrt{\bar{c}_{66}/\rho}$ is introduced for simplification during the following calculation. The present application of second-order approximation is more accurate than the pervious first-order theory, which can be seen form Fig. 2, especially when the mass layer is beyond 2% of the quartz plate's thickness. Sauerbrey's equation provides a simple formula about the frequency shift caused by the additional thin mass layer on the surface of crystal plate, such as $\Delta f=\frac{2f_0^2}{A\sqrt{\rho_Q\mu_Q}}\Delta m$, which can be used to calculate the resonance frequency of QCM. It has been pointed out that the relationship between the resonance frequency and thickness of mass layer is linear by using of this equation [6]. However, in fact this sort of relationship becomes nonlinear, and with the increasing thickness of the mass layer, the tendency of the nonlinearity becomes more and more evident. The second-order approximation can describe this nonlinearity. Thereby, Eq. (17) will be applied in the following discussion.

We define ω_0 as the resonance frequency of fundamental mode without mass layer, which can be calculated from Eq. (18). Once there is an additional mass layer attaching the surface of crystal plate, the frequency will be reduced, as described in Fig. 3. It can be seen from Fig. 3 that the thickness of mass layer $2h'$ has a great effect on the performance of QCM. For some selected mass density, the relationship between the frequency shift $(\omega-\omega_0)$ and thickness ratio is linear, such as Fig. 3(a). To the pointed, when the layer is very thin, the effect of elastic coefficient μ' is insignificant, which can be seen from Fig. 3(b). At the same time, the inertial force plays a leading role in the thickness shear vibration of QCM.

Fig. 4 depicts the variation tendency of non-dimensional frequency shift $\frac{\omega-\omega_0}{\omega_0}$ with the function of the mass density or elastic coefficient of mass layer when h'/h is fixed to 3%. It can be seen from Fig. 4(a) that the absolute value of frequency shift decreases

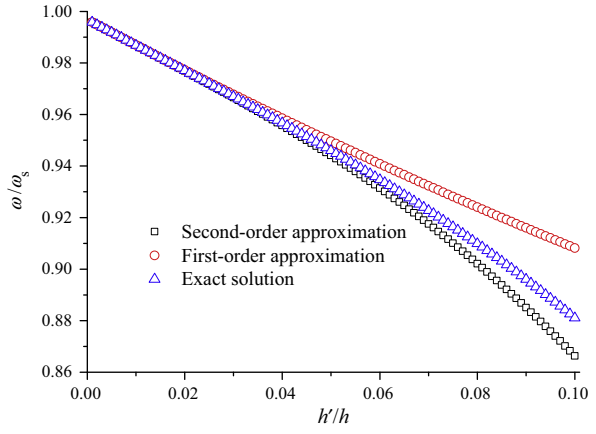

Fig. 2. The frequency comparison calculated by three different equations.

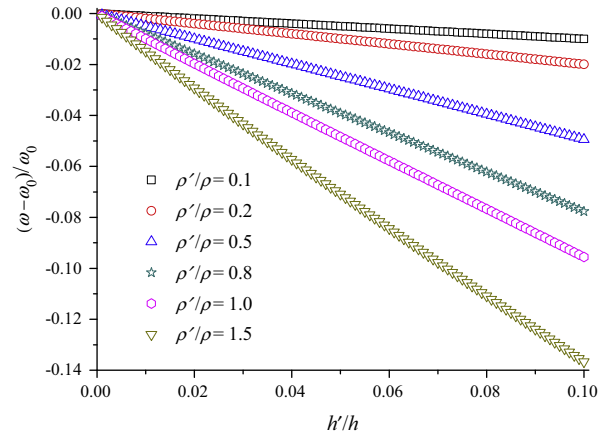

(a) $c_{66} = \mu'$

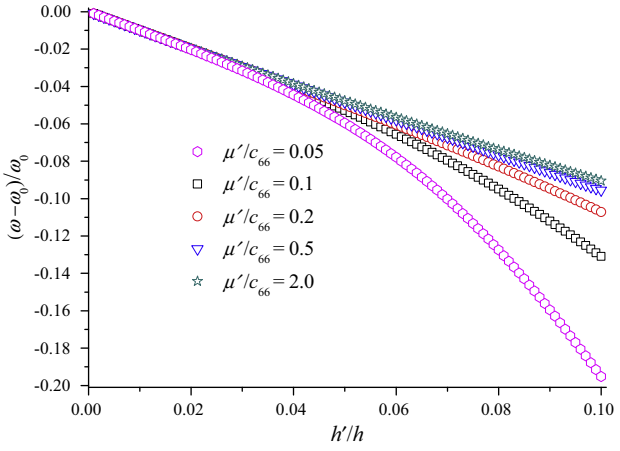

(b) $\rho = \rho'$

Fig. 3. The frequency shift caused by an additional mass layer for some selected μ'/c_{66} and ρ'/ρ.

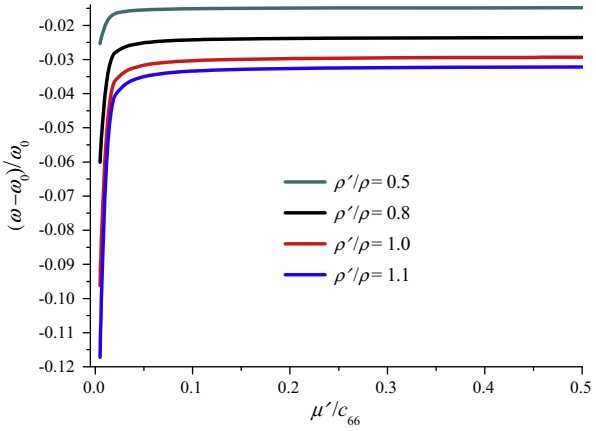

(a) for some selected ρ'/ρ

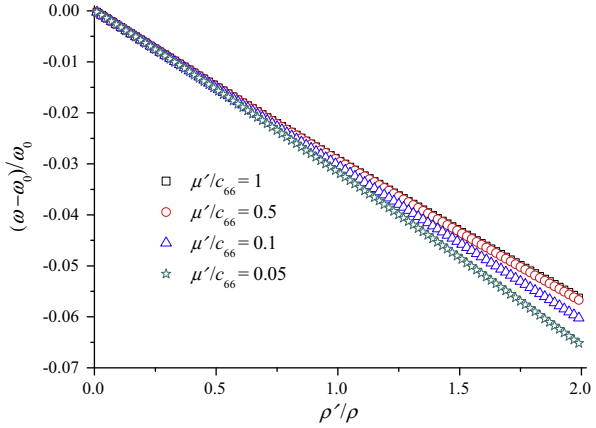

(b) for some selected μ'/c_{66}

Fig. 4. The frequency shift variation of thickness shear vibration when the elastic stiffness or mass density changes (h' = 0.03h).

rapidly when the elastic coefficient μ' increases firstly. When μ' is bigger than $0.1c_{66}$, the fluctuation of resonance frequency is very tiny, which also can be seen from Fig. 4(b). With the increasing of μ', the rigidity of mass layer becomes more and more evident, and the deformation accompanying the crystal plate gradually fades away. This is why these curves are almost keep flat for larger μ'. Oppositely, the relationship between the frequency shift and the mass density of additional mass layer is linear. By comparing Figs. 3(a), 4(a) and (b), it can be concluded that the QCM is more suitable for measuring the thickness and mass density, not the elasticity of additional mass layer, to some extent, owning to the linear relationship in Figs. 3(a) and 4(b).

3.2. Displacement and admittance distributions

Supposing that the external voltage V = 1 V, A_1, A_2, A_3, and A_4 can be solved by using of Eq. (15). According to the expression of electric displacement in Eq. (4), we can get the current per unit area at the surface [4,6]:

$$I = -i\omega\varepsilon_{22}A_3 \exp(i\omega t). \tag{22}$$

The first few resonances of the displacement u_1 and input admittance $I/(2V)$ at $x_2 = h$ versus the driving frequency are shown in Fig. 5. During the simulation in this part, the damp of quartz crystal is introduced by $c_{66} = c_{66} + i\omega\eta_q$ [6]. Here η_q stands for damping factor, and is fixed to 10^{-5}. The corresponding magnitude of displacement is 17.137 μm when the structure is driven in resonant frequency ($\omega = 0.967576\omega_0$) according to our results. As expected, displacement and input admittance assume their own maxima at resonant frequencies, thus indicating that the device is a resonator operating at a particular frequency. However, the magnitude of displacement or input admittance is not zero when the driving frequency is not the resonant frequency. For instance: when external frequency satisfies $\omega = 0.9\omega_0$, the amplitude of excited displacement is 2.067 nm, and if $\omega = 0.965\omega_0$, the amplitude will be 0.512 μm. It should be stressed here that the amplitude of displacement and admittance of even-order mode is smaller than that of odd-order mode. Especially in Fig. 5(b), the second mode cannot be captured from the admittance spectrum. In the opinion of authors, this phenomenon may be due to the fact that the external voltage is anti-symmetric about the middle plane of crystal plate.

The density of mass layer has a great effect on the performance of QCM, as described in Fig. 6. Both the resonance frequency and the peak value have changed for different mass density ρ'. However, the bandwidth at resonance seems to have no relationship with it.

4. Transient effect investigation

In real applications, the external voltage cannot keep constant all the time. Sometimes, incident current or voltage becomes instable for some reason; for instance, a sudden switching-off caused by

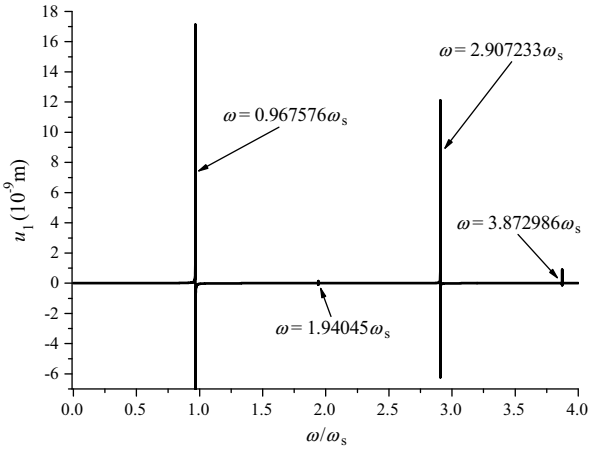

(a) displacement distribution

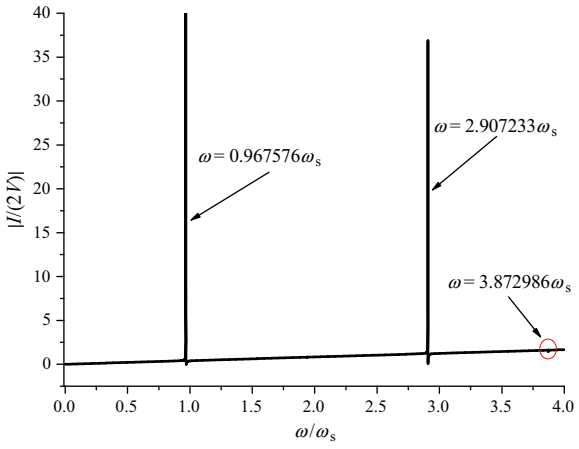

(b) amplitude of admittance

Fig. 5. The first few resonances of the displacement and admittance at $x_2 = h$ versus the driving frequency ($h' = 0.03h$, $\rho' = \rho$, and $\mu' = 0.5c_{66}$).

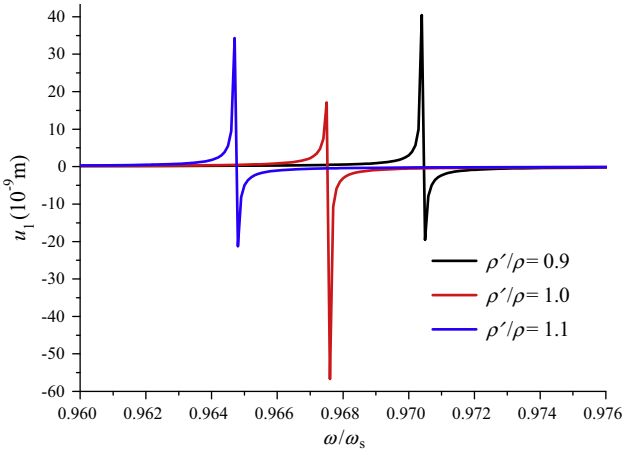

(a) displacement distribution

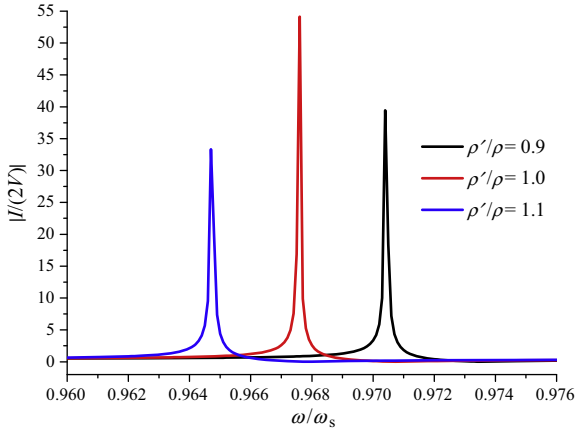

(b) amplitude of admittance

Fig. 6. The effect of mass density of additional mass layer on the first resonance ($h' = 0.03h$, and $\mu' = 0.5c_{66}$).

the thermal and mechanical shocks, which will disturb resonator operation [11–16]. Usually this phenomenon is named as transient effect. Based on the frequency equation, i.e., Eq. (17), we will investigate some transient effects in the QCM in Fig. 1, including the switching on/off processes and under a sudden fluctuation of the driving voltage amplitude or frequency.

Considering the damp of quartz, the governing equation in the AT-cut crystal plate can be described as [14]

$$\bar{c}_{66}\frac{\partial^2 u_1}{\partial x_2^2} + c'_{66}\frac{\partial^3 u_1}{\partial x_2^2 \partial t} = \rho\frac{\partial^2 u_1}{\partial t^2}. \tag{23}$$

Where $c'_{66} = \frac{c_{66}\eta_q}{\omega}$. The initial conditions are assumed as

$$t = 0: \; u_1 = p(x_2), \quad \frac{\partial u_1}{\partial t} = q(x_2). \tag{24}$$

Introducing a linear transformation $u_1 = \hat{u} - \frac{e_{26}}{c_{66}}\frac{V}{2h}x_2$, the governing Eq. (23) can be expressed as

$$\bar{c}_{66}\frac{\partial^2 \hat{u}}{\partial x_2^2} + c'_{66}\frac{\partial^3 \hat{u}}{\partial x_2^2 \partial t} = \rho\frac{\partial^2 \hat{u}}{\partial t^2} - \rho\frac{e_{26}}{c_{66}}\frac{x_2}{2h}\frac{d^2V}{dt^2}. \tag{25}$$

The unknown displacement can be expressed in terms of the following trigonometric series [14]:

$$\hat{u} = \sum_{n=1,3,5}^{\infty} T_n(t)\sin(\xi_n x_2) + \sum_{n=2,4,6}^{\infty} T_n(t)\cos(\xi_n x_2). \tag{26}$$

Similarly, to conveniently solve this problem, we also expand the known linear function of x_2 and the initial conditions $p(x_2)$ and $q(x_2)$:

$$\begin{cases} x_2 = \sum_{n=1,3,5}^{\infty} S_n \sin(\xi_n x_2) + \sum_{n=2,4,6}^{\infty} S_n \cos(\xi_n x_2), \\ p(x_2) = \sum_{n=1,3,5}^{\infty} P_n \sin(\xi_n x_2) + \sum_{n=2,4,6}^{\infty} P_n \cos(\xi_n x_2), \\ q(x_2) = \sum_{n=1,3,5}^{\infty} Q_n \sin(\xi_n x_2) + \sum_{n=2,4,6}^{\infty} Q_n \cos(\xi_n x_2). \end{cases} \tag{27}$$

The undetermined constant S_n, P_n, and Q_n can be calculated by using of orthogonality of trigonometric function, which will not be introduced one by one. Eq. (26) can be changed further:

$$\frac{\partial^2 T_n}{\partial t^2} + \lambda_n'^2\frac{\partial T_n}{\partial t} + \lambda_n^2 T_n = \frac{e_{26}}{c_{66}}\frac{d^2V}{dt^2}\frac{S_n}{2h}. \tag{28}$$

Where $\lambda_n = \xi_n\sqrt{\bar{c}_{66}/\rho}$, $\lambda'_n = \xi_n\sqrt{c'_{66}/\rho}$. Without loss of generality, it is assumed that the inertial voltage satisfies $V = -iV_0\exp(i\omega t)$, with its real parts representing the physical fields. Hereby, the solution of Eq. (28) can be obtained as

$$T_n = C_{1n}\exp(\beta_{1n}t) + C_{2n}\exp(\beta_{2n}t) + \frac{1}{(-\omega^2 + i\omega\lambda_n'^2 + \lambda_n^2)}\frac{e_{26}}{c_{66}}\frac{i\omega^2 V_0}{2h}S_n\exp(i\omega t). \tag{29}$$

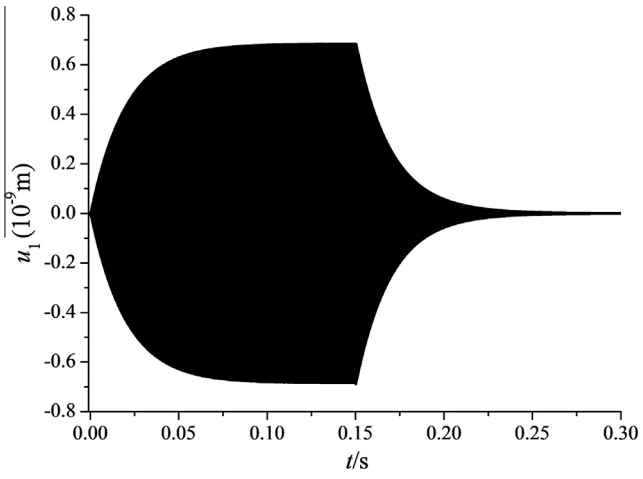

Fig. 7. The amplitude fluctuation when the QCM is turned on at $t = 0$, and then turned off at $t = 0.15$ s ($h' = 0.03h$, $\rho' = \rho$, and $\mu' = 0.5c_{66}$).

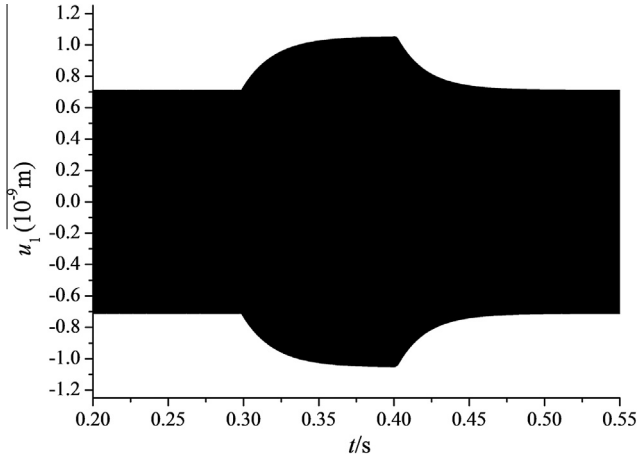

Fig. 8. The amplitude fluctuation when the driving voltage is increased from V to $V + \Delta V$ at $t = 0.3$ s, and decreased back to V at $t = 0.4$ s ($\Delta V = 0.5$ V, $h' = 0.03h$, $\rho' = \rho$, and $\mu' = 0.5c_{66}$).

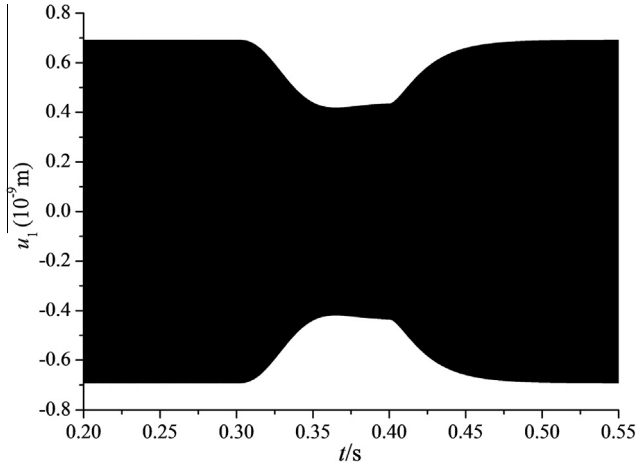

Fig. 9. The amplitude fluctuation when the driving frequency is increased from f to $f + \Delta f$ at $t = 0.3$ s, and decreased back to f at $t = 0.4$ s ($\Delta f = 10$ Hz, $h' = 0.03h$, $\rho' = \rho$, and $\mu' = 0.5c_{66}$).

In which $\beta_{1n} = \frac{-\lambda_n'^2 + \sqrt{\lambda_n'^4 - 4\lambda_n^2}}{2}$, and $\beta_{2n} = \frac{-\lambda_n'^2 - \sqrt{\lambda_n'^4 - 4\lambda_n^2}}{2}$. C_{1n} and C_{2n} are undetermined constants, which need to be calculated by considering the initial conditions described in Eq. (24). The specific computational process has been presented by Liu et al. [14], which has been omitted for simplification in present contribution.

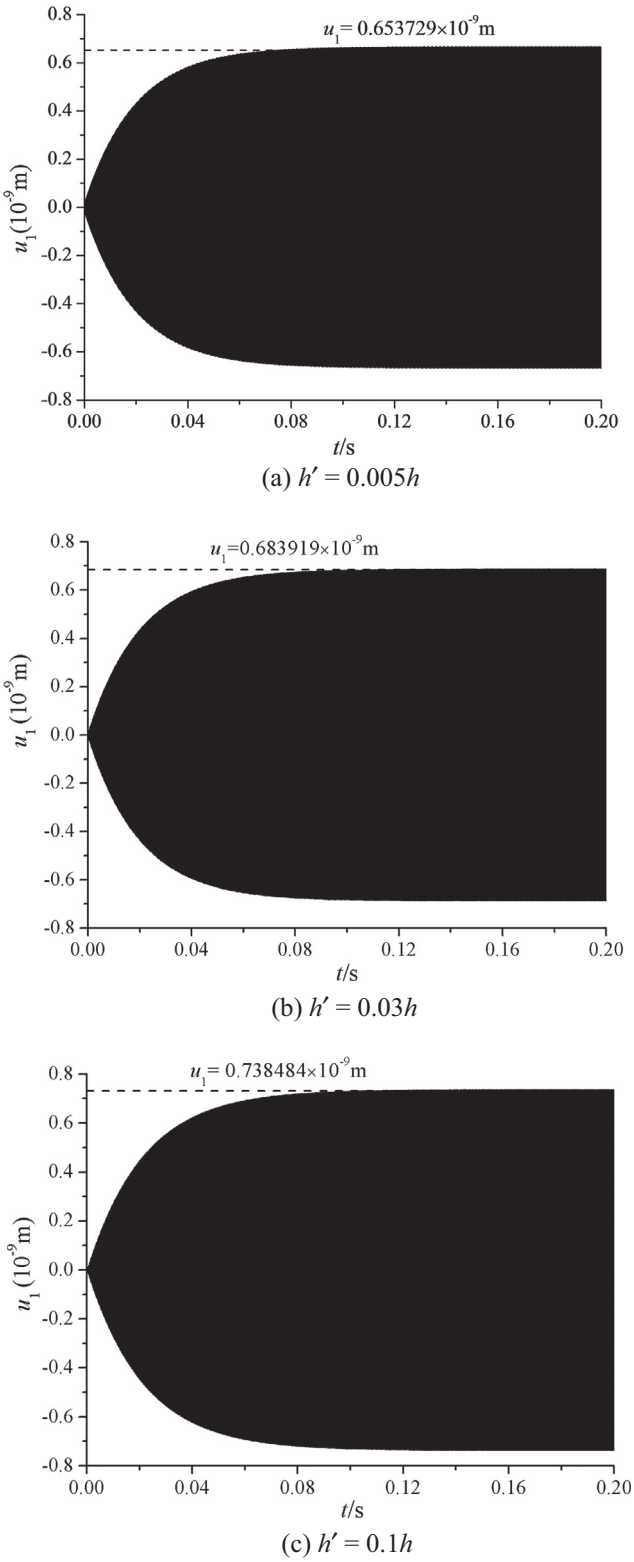

Fig. 10. The effect of thickness of mass layer on the QCM turning on ($\rho' = \rho$, and $\mu' = 0.5c_{66}$): (a) $h' = 0.005h$; (b) $h' = 0.03h$; (c) $h' = 0.1h$.

Fifty terms in the series are kept in the following calculation with twelve significant figures for the displacement field. Meanwhile, the driving frequency of the external voltage is fixed at

$\omega = \omega_1$, where $\omega_1 = 0.967576\omega_s$ ($f = 0.5\omega_1/\pi$) is the frequency of fundamental thickness shear mode with $h' = 0.03h$, $\rho' = \rho$, and $\mu' = 0.5c_{66}$. The amplitude fluctuation of displacement at $x_2 = h$ when the QCM is turned on at $t = 0$, and then turned off at $t = 0.15$ s with the initial conditions $p(x_3) = 0$ and $q(x_3) = 0$ is shown in Fig. 7. In this case, separate theoretical solutions exist in two time intervals of (0,0.15 s) and (0.15 s,∞). The displacement and velocity fields at the end of the first interval serve as the initial conditions for the second interval. The amplitude of the displacement starts from zero, increases monotonically, and then reaches the steady-state vibration during the first interval. After switching off, it will take about 0.1 s for the QCM to come to rest during the second interval.

Another typical transient phenomenon is the sudden fluctuation of external voltage or frequency. It is assumed that the QCM is working normally; suddenly, the driving voltage is increased from V to $V + \Delta V$ at $t = 0.3$ s, and then decreased back to V at $t = 0.4$ s. Fig. 8 gives the corresponding amplitude fluctuation when $\Delta V = 0.5$ V. Besides, the effect of frequency instability with $\Delta f = 10$ Hz off the resonance is shown in Fig. 9. It can be seen from Figs. 8 and 9 that the displacement u_1 of thickness shear mode at $x_2 = h$ is sensitive to the external voltage and frequency. The time scale of the transient processes of amplitude drop and rise is about 0.1 s.

The thickness of additional mass layer has a great influence on the process of switching on for the QCM, which can be seen from Fig. 10. A QCM with a thicker mass layer on its surface will lead to a larger displacement amplitude and longer transient response time.

5. Conclusions

In summary, a second-order approximation of Taylor series has been used to obtain the frequency equation of thickness shear vibration in a QCM containing an infinite AT-cut crystal plate with an isotropic mass layer on its surface. A dispersion equation, which can be reduced as special cases in literature to a few known elastic or quasi-static piezoelectric wave solution, is analytically obtained by using of continuous boundary conditions. The good convergence and high precision of this method have been illustrated. The comprehensive mechanical performance of the QCM has been proceed, including the free vibration analysis, forced vibration excitation by external alternating voltage, and simulation of transient effect. Some numerical examples were provided to illustrate the detailed effect of the mass layer on the mechanical properties of QCM in Fig. 1, which yields the following points:

(1) Comparing with detecting the elastic coefficient of additional mass layer, the QCM is more suitable for measuring the thickness and mass density, to some extent, which is because of the linear relationship between the frequency shift and the change of mass density or thickness.
(2) It should be stressed here that the amplitude of displacement and admittance of even-order mode is much smaller than that of odd-order mode. Hence, the symmetric modes are hardly excited by the external anti-symmetric alternating voltage.
(3) It will take about 0.1 s for the QCM to become stable for encountering a turning-on, switching-off, or the sudden fluctuation of external frequency and voltage. Meanwhile, a QCM with a thicker mass layer on its surface will lead to a larger displacement amplitude and longer transient response time at resonance.

This approximation method applied in the present paper could be used in the study of acoustic waves along other analogous systems with inhomogeneous materials or multilayered structure. Therefore, a higher order approximation needs to be adopted during the analysis, which can provide theoretical guidance in the design of wave propagation in other piezoelectric coupled structures.

Acknowledgments

The National Natural Science Foundation of China (Nos. 11272247, 11402187, 11172226, and 51178390), the National 111 Project of China (No. B06024) and China Postdoctoral Science Foundation funded project (2014M560762) are gratefully acknowledged for their financial support.

Appendix A

The expressions of displacement and stress in additional mass layer can be expressed as

$$\begin{cases} u_1' = [A_1' \cos(\xi' x_2) + A_2' \sin(\xi' x_2)] \exp(i\omega t), \\ T_{12}' = \mu' \xi' [-A_1' \sin(\xi' x_2) + A_2' \cos(\xi' x_2)] \exp(i\omega t). \end{cases} \tag{A1}$$

By using of this expression, the exact frequency equation can be obtained in the following form:

$$\left[k_{26}^2 \sin(\xi h) - \xi h \cos(\xi h)\right] \left[\frac{\mu' \xi'}{\bar{c}_{66} \xi} \cos(\xi h) \sin(2\xi' h') + 2 \sin(\xi h) \cos(2\xi' h')\right] + \xi h \sin^2(\xi h) \frac{\mu' \xi'}{\bar{c}_{66} \xi} \sin(2\xi' h') = 0. \tag{A2}$$

Eq. (A2) can be written in a concise form, such as

$$\left[2 \tan(\xi h) + \frac{\mu' \xi'}{\bar{c}_{66} \xi} \tan(2\xi' h')\right] \left[k_{26}^2 \tan(\xi h) - \xi h\right] + \frac{\mu' \xi'}{\bar{c}_{66} \xi} \xi h \tan^2(\xi h) \tan(2\xi' h') = 0. \tag{A3}$$

Using the relation of $R_0 = \frac{2h'\rho'}{2h\rho} = \frac{\mu' \xi'}{\bar{c}_{66} \xi} \frac{2h' \xi'}{2h \xi}$, Eq. (A2) can be reduced as

$$\left[k_{26}^2 \sin(\xi h) - \xi h \cos(\xi h)\right] \left[2\xi h R_0 \cos(\xi h) \frac{\sin(2\xi' h')}{2\xi' h'} + 2 \sin(\xi h) \cos(2\xi' h')\right] + 2(\xi h)^2 \sin^2(\xi h) R_0 \frac{\sin(2\xi' h')}{2\xi' h'} = 0. \tag{A4}$$

Expanding $\sin(2\xi' h')$ and $\cos(2\xi' h')$ into Taylor series when the thickness of upper layer is very thin, we can get

$$\sin(2\xi' h') = 2\xi' h' - \frac{(2\xi' h')^3}{3!} + (-1)^m \frac{(2\xi' h')^{2m-1}}{(2m-1)!} + \ldots,$$
$$\cos(2\xi' h') = 1 - \frac{(2\xi' h')^2}{2!} + (-1)^m \frac{(2\xi' h')^{2m}}{(2m)!} + \ldots. \tag{A5}$$

In present contribution, we only consider the second-order approximation of Taylor series for simplification. Hence, $\sin(2\xi' h')$ and $\cos(2\xi' h')$ can be replaced approximately by $2\xi' h'$ and $[1 - 2(\xi' h')^2]$, respectively. Based on this approximation, Eq. (A4) can be equal to

$$\left[k_{26}^2 \sin(\xi h) - \xi h \cos(\xi h)\right] \left\{2\xi h R_0 \cos(\xi h) + 2 \sin(\xi h) \left[1 - 2(\xi' h')^2\right]\right\} + 2(\xi h)^2 \sin^2(\xi h) R_0 = 0. \tag{A6}$$

In fact, Eq. (A6) is the same as Eq. (17).

References

[1] G.Z. Sauerbrey, Use of quartz vibrator for weighing thin films on a microbalance, Z. Phys. 155 (1989) 206–222.
[2] P.J. Cumpson, M.P. Seah, The quartz crystal microbalance: radial/polar dependence of mass sensitivity both on and off the electrodes, Meas. Sci. Technol. 1 (1990) 544–555.

[3] B.A. Martin, H.E. Hager, Velocity profile on quartz crystals oscillating in liquids, J. Appl. Phys. 65 (1989) 2630–2635.
[4] K.K. Kanazawa, Mechanical behaviour of films on the quartz microbalance, Faraday Discuss. 107 (1997) 77–90.
[5] J.R. Vig, A. Ballato, Comments on the effects of nonuniform mass loading on a quartz crystal microbalance, IEEE Trans. Ultrason. Ferroelect. Freq. Control 45 (1998) 1123–1124.
[6] F. Lu, H.P. Lee, S.P. Lim, Mechanical description of interfacial slips for quartz crystal microbalances with viscoelastic liquid loading, Smart Mater. Strut. 12 (2003) 881–888.
[7] J.M. Stephen, E.G. Victoria, C.F. Gregory, Characterization of a quartz crystal microbalance with simultaneous mass and liquid loading, Anal. Chem. 63 (1991) 2272–2281.
[8] P. Bovik, A comparison between the Tiersten model and O(H) boundary conditions for elastic surface waves guided by thin layers, J. Appl. Mech. Trans. ASME 63 (1996) 162–167.
[9] N. Liu, J.S. Yang, W.Q. Chen, Effects of a mass layer with gradually varying thickness on a quartz crystal microbalance, IEEE Sens. J. 11 (2011) 1635–1639.
[10] J.S. Yang, H.G. Zhou, W.P. Zhang, Thickness-shear vibration of rotated Y-cut quartz plates with relatively thick electrodes of unequal thickness, IEEE Trans. Ultrason. Ferroelect. Freq. Control 52 (2005) 918–922.
[11] V.M. Bazhenov, A.F. Ulitko, Investigation of the dynamic behavior of a piezoelectric ceramic layer during instantaneous electric loading, Int. Appl. Mech. 11 (1975) 16–20.
[12] N.A. Shulga, L.O. Grigoreva, Method of characteristics in analysis of the propagation of electroelastic thickness oscillations in a piezoceramic layer under electric excitation, Int. Appl. Mech. 44 (2008) 1093–1097.
[13] R.Y. Zhang, H.P. Hu, A few transient effects in AT-cut quartz thickness-shear resonators, IEEE Trans. Ultrason. Ferroelect. Freq. Control 58 (2011) 2758–2762.
[14] N. Liu, J.S. Yang, F. Jin, Transient thickness-shear vibration of a piezoelectric plate of monoclinic crystals, Int. J. Appl. Electrom. 38 (2012) 27–37.
[15] Z. Wang, M.H. Zhao, J.S. Yang, Amplitude evolution equation and transient effects in piezoelectric crystal resonators, J. Appl. Phys. 114 (2013) 144510.
[16] J.N. Wang, Y.T. Hu, J.S. Yang, Frequency spectra of AT-cut quartz plates with electrodes of unequal thickness, IEEE Trans. Ultrason. Ferroelect. Freq. Control 57 (2010) 1145–1151.
[17] P.C. Vinh, V.T.N. Anh, V.P. Thanh, Rayleigh waves in an isotropic elastic half-space coated by a thin isotropic elastic layer with smooth contact, Wave Motion 51 (2014) 496–504.
[18] H.F. Tiersten, Thickness vibrations of piezoelectric plates, J. Acoust. Soc. Am. 34 (1963) 53–58.
[19] Z.T. Yang, S.H. Guo, Y.T. Hu, J.S. Yang, Thickness-shear vibration of rotated Y-cut quartz plates with unattached electrodes and asymmetric air gaps, Philos. Mag. Lett. 89 (2009) 313–321.
[20] P. Li, F. Jin, Effect of an imperfect interface in a quartz crystal microbalance for detecting the properties of an additional porous layer, J. Appl. Phys. 115 (2014) 054502.
[21] H.F. Tiersten, Linear Piezoelectric Plate Vibrations, Plenum, New York, 1969.
[22] A.N. Abdalla, F. Alsheikh, A.Y. Al-Hossain, Effect of initial stresses on dispersion relation of transverse waves in a piezoelectric layered cylinder, Mater. Sci. Eng. B – Adv. 162 (2009) 147–154.